BIOCHEMISTRY
including biophysical chemistry & molecular biology

Article

pubs.acs.org/biochemistry

# Noncooperative Metalation of Metallothionein 1a and Its Isolated Domains with Zinc

Duncan E. K. Sutherland, Kelly L. Summers, and Martin J. Stillman*

Department of Chemistry, The University of Western Ontario, London, Ontario, Canada N6A 5B7

**ABSTRACT:** Mammalian metallothioneins (MTs) are a family of small cysteine-rich proteins capable of binding 7 $Zn^{2+}$ or $Cd^{2+}$ ions into two distinct domains: an N-terminal $\beta$-domain that binds 3 $Zn^{2+}$ or $Cd^{2+}$ and a C-terminal $\alpha$-domain that binds 4 $Zn^{2+}$ or $Cd^{2+}$. MT has been implicated in a number of physiological functions, including metal ion homeostasis, toxic metal detoxification, and as a protective agent against oxidative stress. Conventionally, MT has been understood to coordinate metal ions in a cooperative fashion. Under this mechanism of metalation, the only species of biological relevance would be the metal-free (apo-) form of the protein and the fully metalated (holo-) form of the protein. However, an increasing body of evidence suggests that metalation occurs in a noncooperative manner. If this latter mechanism is correct, then partially metalated forms of the protein will be stable and able to take part in cellular chemistry. We report in this paper conclusive evidence that shows that biologically essential zinc binds to MT in a noncooperative manner. In addition, we report for the first time the stability of a $Zn_5$-MT species. The implications of these findings are discussed in terms of the mechanism of metalation.

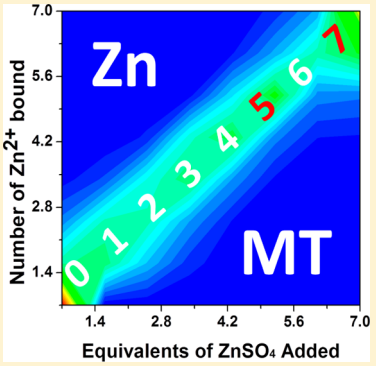


Metallothioneins (MTs) are a family of small cysteine-rich proteins that are found in all organisms and have been implicated in toxic metal detoxification, metal-ion homeostasis, and as a protective agent against oxidative stress. Using its thiolate groups, MT is able to coordinate a variety of metals including $Cu^{+}$, $Ag^{+}$, $Au^{+}$, $Zn^{2+}$, $Cd^{2+}$, $Hg^{2+}$, $As^{3+}$, and $Pt^{2+/4+}$.[1−3] These metal ions are capable of coordinating in a number of geometries, including digonal, trigonal, and tetrahedral.[4] For $Zn^{2+}$ coordination, a tetrahedral geometry is adopted via a mixture of terminal and bridging cysteine residues. Processes that MT has been implicated in rely on its dynamic ability to bind and release metal ions within the cellular environment. However, the majority of MT research to date has focused on the fully metalated forms of the protein and to a lesser extent the metal-free form.[3,4]

The most well-characterized members of the MT family are the mammalian MTs (Figure 1). Both X-ray diffraction and NMR studies of the fully metalated mammalian protein show that metal ions form two essentially isolated and distinct metal−thiolate clustered binding domains using the 20 cysteine residues of the protein. In mammalian MT, Zn-MT is the dominant form; however, Cu-MT has also been isolated from several sources including fetal liver MT, bovine calf liver MT, rat kidney, and brain-specific MT-3.[3] Structurally, mammalian MT can be subdivided into two domains: the N-terminal $\beta$-domain, which is capable of binding 3 $Zn^{2+}$, 3 $Cd^{2+}$, or 6 $Cu^{+}$ metal ions using 9 cysteine residues, and the C-terminal $\alpha$-domain, which is capable of binding 4 $Zn^{2+}$, 4 $Cd^{2+}$, or 6 $Cu^{+}$ metal ions using 11 cysteine residues.[5−7] The current view of these domains is that each acts as an effectively isolated metal−thiolate cluster. This view has been supported by a number of NMR studies of mammalian MT, where no interdomain NOEs were found.[7,8] Since NOEs are a through space phenomenon, it has been inferred that the two domains are not physically near one another. The sole exception to this observation is supermetalation of MT, where addition of excess $Cd^{2+}$ results in formation of a single $Cd_8Cys_{20}$ "superdomain".[9,10]

It has been suggested that the existence of the two domain structure present in many MTs allows the protein to function simultaneously in both $Zn^{2+}$ and $Cu^{+}$ chemistries.[11,12] The potential for MT to spatially separate metal ion chemistry into different domains has significant consequences for our understanding of the role of MT in metal ion homeostasis and as a protective agent against oxidative stress. For instance, MT-3 has been proposed to play an important role in maintaining the balance of metals in the brain,[13] and it has been reported to be downregulated in patients with Alzheimer's disease. A recent paper has shown that $Zn_7$-$\beta\alpha$-MT 3 is capable of metal exchange with the copper bound amyloid-$\beta$-peptide ($A\beta_{1-40}$-$Cu^{2+}$).[14] The exchange reaction and subsequent reduction to $Cu^{+}$ leads to the formation of $Cu_4Zn_4$-$\beta\alpha$-MT 3. This process eliminates the production of reactive oxygen species and related toxic effects, which may provide some protection against Alzheimer's disease. Metallothioneins are considered to play such important roles in the homeostasis of $Zn^{2+}$ that an understanding of the metalation chemistries of the full MT protein and the possible roles of the two domains is necessary.

Currently, little is known about the exact mechanism of the metalation of MT. The conventional view is that MT likely metalates in a cooperative "all or nothing" fashion. If this is the case, then the only stable species will be the fully metalated and

**Received:** April 9, 2012
**Revised:** July 12, 2012
**Published:** July 23, 2012





dx.doi.org/10.1021/bi3004523 | *Biochemistry* 2012, 51, 6690−6700

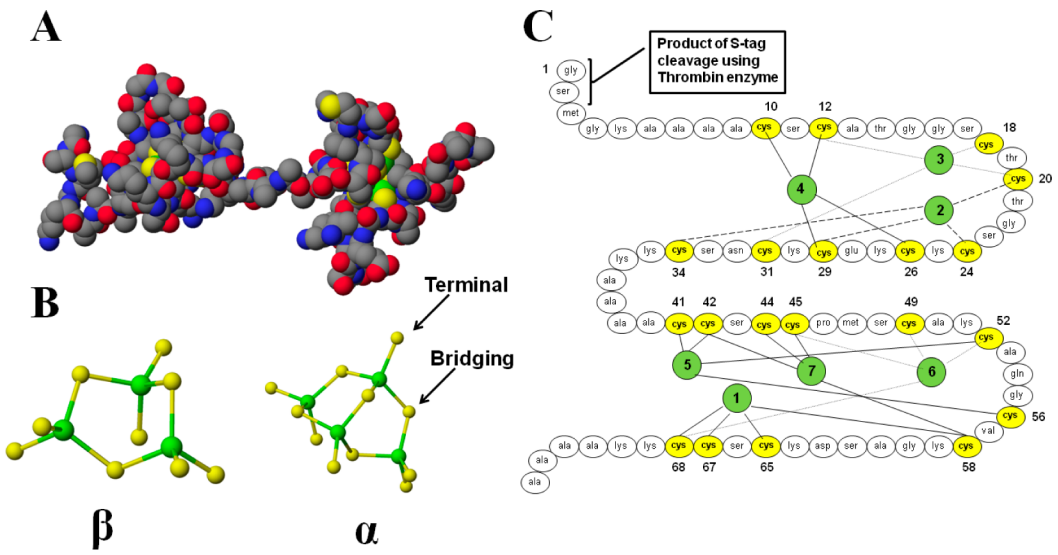


**Figure 1.** Three-dimensional structure and sequence-metal-binding alignment of $Cd_7$-MT 1a. (A) A space-filling structure of $Cd_7$-$\beta\alpha$-rhMT 1a. The N-terminal $\beta$-domain is located on the left-hand side, while the C-terminal $\alpha$-domain is located on the right-hand side. (B) Cadmium-cysteinyl-thiolate clusters of $Cd_7$-$\beta\alpha$-rhMT 1a presented as ball and stick models: $\beta$-domain (left) and $\alpha$-domain (right). (C) A metal connectivity diagram for MT 1a based on the sequence and the presence of 7, tetrahedrally coordinated metals. Each of the seven cadmium atoms is connected to exactly four cysteine amino acids. The connectivity diagram has been renumbered from the original to accommodate the amino acids glycine and serine, both of which are a product of S-tag cleavage with thrombin, located on the N-terminal of the $\beta$-domain. Numbering of the Cd-thiolate centers is based on the NMR assignment by Messerle et al.[7] Data from Chan et al. were used to produce the molecular models seen in (A) and (B).[15]

metal free forms of the protein. The unmetalated form with its 20 cysteine thiols would be highly susceptible to oxidation, and any partially metalated forms would also be unstable and susceptible to oxidation of the free cysteine thiols. A number of acid-induced demetalation studies of MT have suggested that demetalation of the two clusters occurs as a two-step cooperative process with each individual step resulting in complete loss of the metal ions bound in one of the two clusters.[15−18] That is, sequential demetalation of the clusters occurs rather than demetalation involving metals from both clusters. This model strongly suggests that acid induced loss of a single metal ion destabilizes the cluster enhancing complete metal ion removal. Contrasting clustered loss of metal ions, other studies have suggested that MT is capable of donating fractional amounts of its full metal ion load to $Zn^{2+}$-depleted apo-enzymes, while oxidizing agents have also been shown to be capable of labilizing some of the $Zn^{2+}$ ions found in MT.[19,20] These conclusions profoundly impact our understanding of the stability of the fully metalated clusters and their biologically important chemistries; however, the model depends entirely on the ability of the instrumental analysis to monitor partial metalation.

Until the advent of electrospray ionization mass spectrometry (ESI-MS), many of the spectroscopic techniques available provided only an averaged signal of all species present in solution. Consequently, researchers assumed uniform metalation of all MT proteins and that the stoichiometric equivalents of metal ions added to solution directly corresponded to the precise and nominally exact metalation status of the protein being studied. Unique to ESI-MS is its ability to determine not only the number of metals bound but also the identities of the metals bound, which allows for a direct correlation between the spectroscopy and speciation of a sample. ESI-MS studies have provided a wealth of new data concerning both demetalation and metalation for a range of metals with respect to MT proteins from different sources. Studies of the mechanism of metalation of mammalian MT for $Cu^+$ ions were considered to show cooperativity, at least for the first 4 metal ions of a possible 12 $Cu^+$ ions.[21] In addition, MT isoform 2 has been shown to metalate $Zn^{2+}$, $Cd^{2+}$, and $Cu^+$ in a cooperative fashion.[22]

To further investigate the mechanism of metalation, we have previously taken advantage of the discriminating power of ESI−mass spectrometry to demonstrate that the partially metalated forms of MT isoform 1 are stable for both $Cd^{2+}$ and $As^{3+}$.[2,23−25] By measuring the masses of all species in solution, ESI−mass spectrometry provides the stoichiometric ratios of all the differently metalated species. This new information completely changes our perspective of the metalation reaction because it allows immediate and precise determination of the mechanism of all metalation reactions. As a consequence, the observation of stable partially metalated MTs during the ESI-MS metalation experiments with $Cd^{2+}$ and $As^{3+}$ supported metalation occurring in a noncooperative fashion. In a noncooperative mechanism of metalation, the binding affinity of MT for metal ions is directly dependent upon the number of available metal-binding sites, and the binding affinity decreases for each successive metalation event in the normal and expected pattern of coordination chemistry.[3,26] This means that in the absence of excess metal ions the last metal binding site might not be occupied, leading to a partially metalated species. The kinetic data of Ngu et al. provided clear evidence for this effect[2,25,27,28] because the series of specific rate constants determined from the time-dependent data diminished for each successive metal bound up the sixth $As^{3+}$.

Knowing the exact metalation status of Zn-MT is vital for the correct interpretation of MT's role as both a donor of $Zn^{2+}$ ions to apo-proteins and in its role in the redox chemistry of the cell.[29] With its 20 thiol groups, MT has long been thought of as a protective agent against oxidative stress. In this role, Zn-MT interacts with an oxidant, such as $H_2O_2$, and is oxidized. This then leads to the release of $Zn^{2+}$ ions. These free $Zn^{2+}$ ions then


dx.doi.org/10.1021/bi3004523 | *Biochemistry* 2012, 51, 6690−6700

interact with the metal regulatory transcription factor 1 (MTF-1), which translocates from the cytoplasm into the nucleus and upregulates the production of MT.[30] The net effect is that the cell is able to deactivate incoming oxidants.

This brings us to the question of the metalation mechanism for Zn-MTs. If metalation occurs in a noncooperative fashion, then MT may exist as a dynamic antioxidant, where sequential release of each metal ion becomes less favorable as the association constant ($K_F$) of the leaving $Zn^{2+}$ ion increases. Such equilibrium data have recently been reported by Krezel and Maret, who have shown that there are at least three zinc association constants for MT ranging from log($K_F$) values of 11.8 for the first four $Zn^{2+}$ ions bound to ~10 for the fifth and the sixth $Zn^{2+}$ ions and finally to 7.7 for the final $Zn^{2+}$ ion bound.[31]

In this paper, we report on the mechanism of the stepwise metalation of apo-hMT 1a with $Zn^{2+}$ using the metal-free isolated apo-$\beta$-rhMT 1a and apo-$\alpha$-rhMT 1a fragments and the metal-free full protein apo-$\beta\alpha$-rhMT 1a. Individual titrations of both the isolated domains and the full MT protein clearly demonstrate that $Zn^{2+}$ metalation occurs in a noncooperative manner. These results establish that one of the two key metals in the biological chemistry of metallothionein binds non-cooperatively. This allows studies of the biological role of MT to be advanced on a secure foundation; the metalation and demetalation equilibria control the biological function of metallothioneins.

## EXPERIMENTAL METHODS

**Chemicals.** Cadmium sulfate (Fisher Scientific), zinc sulfate (Caledon Laboratory Chemicals), ThrombinCleanCleave Kit (Sigma), Tris, tris(hydroxymethyl)aminomethane (EMD Chemicals/VWR), ammonium hydroxide (Caledon Laboratory Chemicals), formic acid (Caledon Laboratory Chemicals), and hydrochloric acid (Caledon Laboratory Chemicals). All solutions were made with >16 MΩ·cm deionized water (Barnstead Nanopure Infinity). HiTrap SP HP ion exchange columns (Amersham Biosciences/GE Healthcare), superfine G-25 Sephadex (Amersham Biosciences/GE Healthcare), and stirred ultrafiltration cell Model 8200 (Amicon Bioseparations/Millipore) with a YM-3 membrane (3000 MWCO) were used in protein preparation steps.

**Protein Preparation.** The expression and purification methods have been previously reported.[15] $\beta$-rhMT 1a, $\alpha$-rhMT 1a, and $\beta\alpha$-rhMT 1a proteins used in this study were based on the 38-residue, 41-residue, and 72-residue sequences, respectively: $\beta$-rhMT 1a MGKAAAACSC ATGGSCTCTG SCKCKECKCN SCKKAAAA, $\alpha$-rhMT 1a MGKAAAACCS CCPMSCAKCA QGCVCKGASE KCSCCKKAAA A, $\beta\alpha$-rhMT 1a MGKAAAACSC ATGGSCTCTG SCKCKECKCN SCKKAAAACC SCCPMSCAKC AQGCVCKGAS EKCSCCKKAA AA. There are 9, 11, and 20 cysteine residues present in $\beta$-rhMT 1a, $\alpha$-rhMT 1a, and $\beta\alpha$-rhMT 1a, respectively, and no disulfide bonds. The expression system included, for stability purposes, an N-terminal S-tag (MKETAAAKFE RQHMDSPDLG TLVPRGS). Recombinant proteins were expressed in BL21(DE3) *Escherichia coli*. All cell lines were transformed using the pET29a plasmid. Removal of S-tag was performed using a Thrombin CleanCleave Kit (Sigma). To impede oxidation of the cysteine residues to disulfide bonds, all protein samples were argon saturated and rigorously evacuated. Concentrated hydrochloric acid was used to demetallate protein samples, followed by desalting on a G-25 (Sephadex) column. Unless specifically stated otherwise, all data discussed in this paper are from the same, recombinant, human MT isoform 1a with the specific sequence shown above and will be referred to as "rhMT".

**ESI MS Procedures.** Protein solutions were prepared in dilute formic acid in deionized water (pH 2.7). Final ESI-MS solutions were pH adjusted using concentrated ammonium hydroxide. Protein concentrations were determined by remetalation of a portion of the sample with $Cd^{2+}$ ions, and the Cd-MT was monitored by UV absorption spectroscopy using the absorbance at 250 nm, which corresponds to the ligand-to-metal charge transfer transition generated by the cadmium−thiolate bond ($\varepsilon_{\beta 250}$ = 36 000 $M^{-1}$ $cm^{-1}$; $\varepsilon_{\alpha 250}$ = 45 000 $M^{-1}$ $cm^{-1}$; $\varepsilon_{\beta\alpha 250}$ = 89 000 $M^{-1}$ $cm^{-1}$). Zinc sulfate was prepared in deionized water. Zinc sulfate and all molar equivalents were measured through calibration of the $Zn^{2+}$ content in solution using atomic absorption spectrometry (AAS). The metalation of MT with $Zn^{2+}$ has been previously reported to occur in less than 4 ms.[32] Therefore, the metalation of MT with $Zn^{2+}$ can be considered to be instantaneous. To ensure that the thermodynamic product was observed, each sample was allowed to equilibrate ~3 min between additions of $ZnSO_4$.

All data were collected on an electrospray-ionization time-of-flight (ESI-TOF) micrOTOF II mass spectrometer (Bruker Daltonics) in the positive ion mode. NaI was used as the calibrant. The scan conditions for the spectrometer were as follows: end plate offset, −500 V; capillary, +4200 V; nebulizer, 2.0 bar; dry gas flow, 8.0 L/min; dry temperature, 80 °C; capillary exit, 180 V; skimmer 1, 22.0 V; hexapole 1, 22.5 V; hexapole RF, 600 $V_{pp}$; skimmer 2, 22 V; lens 1 transfer, 88 $\mu$s; lens 1 pre pulse storage 23 $\mu$s. The range was 500.0−3000.0 $m/z$, averaging 2 × 0.5 Hz. Spectra were deconvoluted using the Bruker Compass DataAnalysis software package.

## RESULTS

**Noncooperative Metalation of Isolated Apo-$\beta$-rhMT 1a by $Zn^{2+}$.** The mass spectral data recorded during the titration apo-$\beta$-rhMT with $Zn^{2+}$ are shown in Figure 2 with their corresponding deconvoluted spectra (right-hand column). Stepwise metalation of apo-$\beta$-rhMT (Figure 2A−E) leads to the formation of partially metalated species ($Zn_1$-$\beta$-rhMT, $Zn_2$-$\beta$-rhMT) at substoichiometric equivalents ($\beta$ < 3 $Zn^{2+}$). Complete metalation occurs when 3.5 equiv of $Zn^{2+}$/$\beta$-rhMT is added to solution. It should be noted that one would expect complete metalation to occur at exactly 3 $Zn^{2+}$ added to the apo-$\beta$-rhMT; however, we attribute the discrepancy in the equivalents needed for complete metalation to be the result of slight errors in the estimations of the metal-free protein concentrations as well as from the formation of low concentrations of $Zn(OH)_2$. From the data it can be clearly seen that the dominant metalation state is a direct result of the number of equivalents of $Zn^{2+}$ added to solution. At 1.7 equiv of $Zn^{2+}$ the dominant species is $Zn_1$-$\beta$-rhMT, while at 2.6 equiv of $Zn^{2+}$ the two most abundant species are fully metalated $Zn_3$-$\beta$-rhMT and partially metalated $Zn_2$-$\beta$-rhMT. Metal-free apo-$\beta$-rhMT exhibits charge states corresponding to 4+, 3+, and 2+ at 0.1 equiv of $Zn^{2+}$. The charge state distribution is related to both the number of basic sites on the protein and the surface area of the exposed protein.[33,34] The greater the number of available basic sites for protonation, the greater the overall maximum charge of the protein that is possible. A larger protein (one that occupies a significantly greater volume) is able to


dx.doi.org/10.1021/bi3004523 | *Biochemistry* 2012, 51, 6690−6700

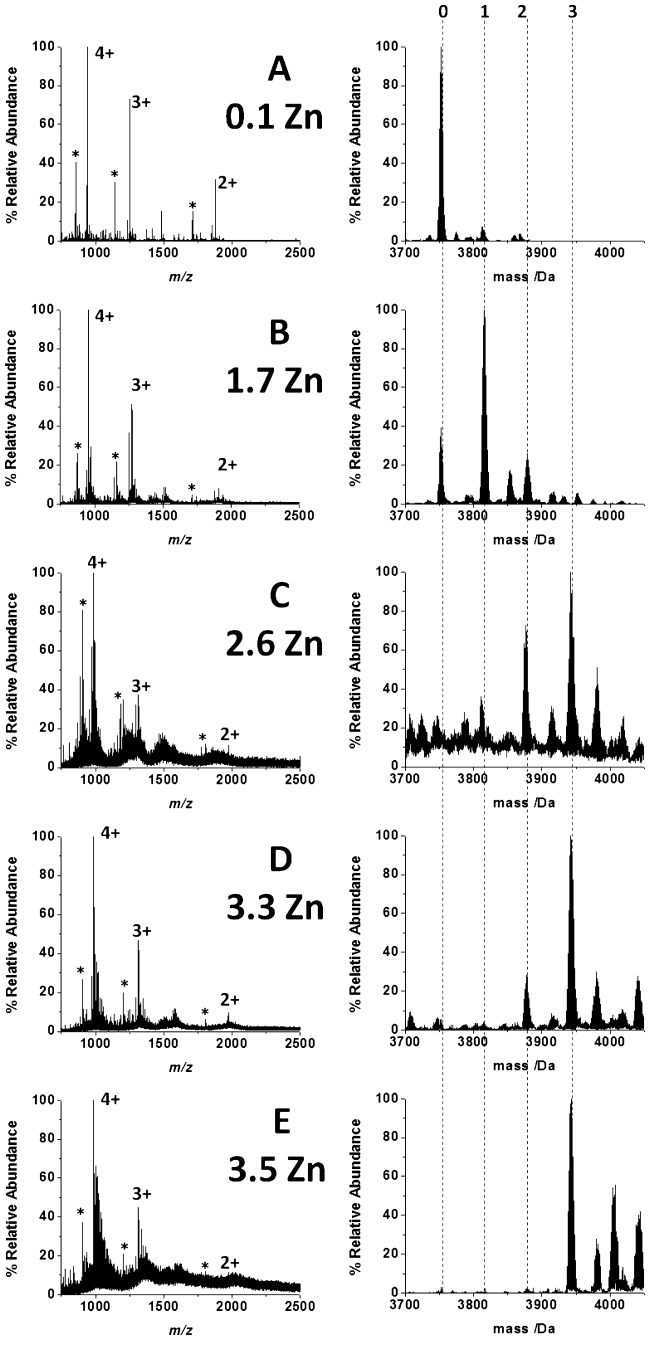


**Figure 2.** ESI mass spectra recorded during the titration of (A-E) apo-$\beta$-rhMT 1a, 29.2 $\mu$M at pH 9.2, with $ZnSO_4$. Spectral changes were recorded as aliquots of Zn(II) (7.3 mM) were added into the solutions on ice. Dotted lines follow metal binding. ESI mass spectral data (left) and their deconvoluted counterparts (right) were recorded at Zn(II) molar equivalents of 0.1, 1.7, 2.6, 3.3, and 3.5. Metalation in excess of $Zn_3$-$\beta$-rhMT is a result of nonspecific adducts.

support more positive charge, since electrostatic interactions are minimized. When a protein folds, both the number of exposed basic sites and the overall volume of the protein decrease, leading to a decrease in both the maximum supportable charge and the total number of supportable charge states. The most significant change in the charge state profile is the decrease in intensity of the 2+ charge state at 1.7 equiv of $Zn^{2+}$ added to solution. There is also a 20% decrease in the intensity of the 3+ relative to the 4+ charge state when comparing apo-$\beta$-rhMT to $Zn_3$-$\beta$-rhMT. We should note at this point that several ESI-MS studies, specifically the kinetic analysis of arsenic metalation,[2,25,27,28] provide strong evidence that the ionization potential of MT, and its isolated domains, are similar for all metalation states (from apo-MT to fully metalated MT), and, therefore, the deconvoluted spectra are good approximations of the actual metal ion distribution in solution. Taken together, these results suggest that the addition of the first two metal ions stabilize a slightly more open conformation of apo-$\beta$-rhMT.

We have assembled the relative abundances of each metalated $\beta$-rhMT species (Figure 2) into Figure 3, which clearly demonstrates that partial metalation occurs; hence, the extent of metalation is directly dependent on the amount of

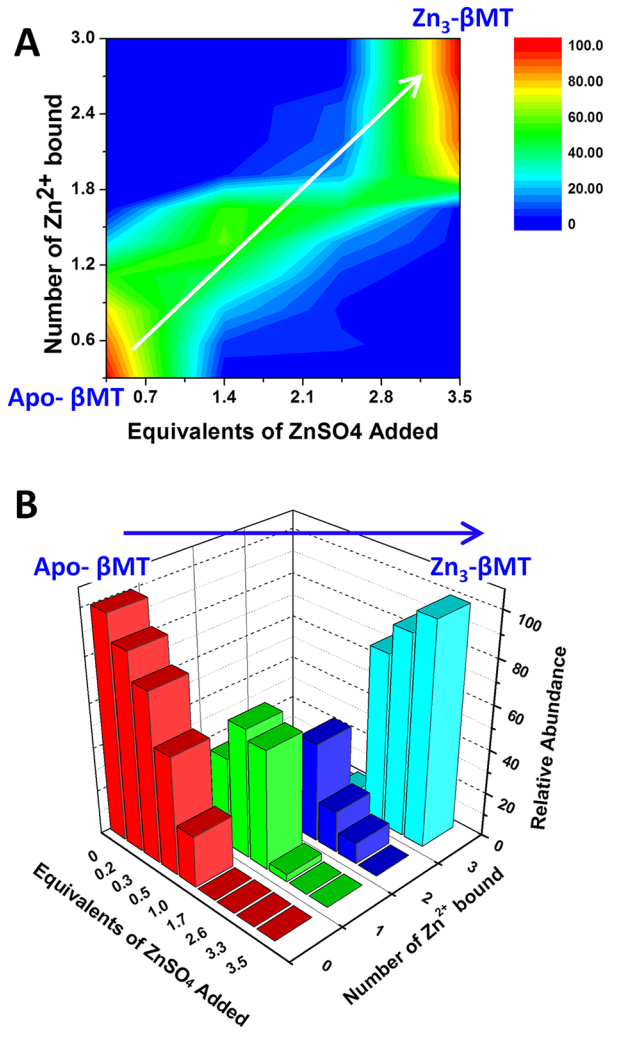


**Figure 3.** Contour and bar graph representation of the metalation state of $\beta$-rhMT 1a as a function of Zn(II) added. (A) A top-down view of metalation, showing the linear progression from apo-$\beta$-rhMT to $Zn_3$-$\beta$-rhMT as a function of $Zn^{2+}$ added to solution. The adjacent legend ranges between 100% abundance (red) and 0% abundance (dark blue). (B) A side-on view of metalation, which shows the relative abundance of each species as a function of $Zn^{2+}$ added to solution. Color code: apo-$\beta$-rhMT is red; $Zn_1$-$\beta$-rhMT is green; $Zn_2$-$\beta$-rhMT is dark blue; $Zn_3$-$\beta$-rhMT is light blue. In both (A) and (B), as the total amount of $Zn^{2+}$ added to the solution of apo-$\beta$-rhMT 1a is increased, the number of metals bound to $\beta$-rhMT 1a also increases. This graph is based upon the deconvoluted mass spectral data shown in Figure 2.


dx.doi.org/10.1021/bi3004523 | Biochemistry 2012, 51, 6690−6700

$Zn^{2+}$ in solution. This must result from a decreased binding affinity of the cysteine thiols for the last $Zn^{2+}$ to be bound. Figure 3A shows a top-down view of the linear progression of the metalation from apo-$\beta$-rhMT to $Zn_3$-$\beta$-rhMT. This linearity is important because it demonstrates that metalation occurs in a noncooperative manner, where the declining affinity of $Zn^{2+}$ for $\beta$-rhMT is directly related to the number of available metal-binding sites. Figure 3B demonstrates that at each equivalent of zinc, with the exception of the beginning and end of the titration, the $\beta$-rhMT exists as a mixture of metalated states. At low equivalents of $Zn^{2+}$ only partially metalated species are observed, while at excess equivalents (>3 equiv of $Zn^{2+}$) only the fully metalated $\beta$-rhMT is observed.

**Noncooperative Metalation of Isolated Apo-$\alpha$-rhMT 1a by $Zn^{2+}$.** Stepwise metalation of apo-$\alpha$-rhMT in Figure 4A–E leads to the formation of partially metalated species ($Zn_1$-$\alpha$-rhMT, $Zn_2$-$\alpha$-rhMT, $Zn_3$-$\alpha$-rhMT) at substoichiometric equivalents ($\alpha$ < 4 $Zn^{2+}$). The dominant metalation state is a direct result of the number of equivalents of $Zn^{2+}$ added to solution. At 2.2 equiv of $Zn^{2+}$ the dominant species is $Zn_1$-$\alpha$-rhMT, while at 3.7 and 3.9 equiv of $Zn^{2+}$ the dominant species are $Zn_2$- and $Zn_3$-$\alpha$-rhMT, respectively. Complete metalation is observed at 4.1 equiv of $Zn^{2+}$ added to solution; however, there is still a relatively small (~15% of total species present) population of $Zn_3$-$\alpha$-rhMT, which we attribute to slight errors in the calculation of the equivalents of $Zn^{2+}$ added. It should be noted that one would expect complete metalation to occur at 4 $Zn^{2+}$ for apo-$\alpha$-rhMT, and like the case for the $\beta$-fragment, we recognize the effect of both analytical errors in concentrations and competitive formation of $Zn(OH)_2$. Much like the $\beta$-domain, apo-$\alpha$-rhMT exhibits significant changes in the distribution of the intensities of 4+, 3+, and 2+ charge states when even a low stoichiometric ratio of $Zn^{2+}$ has been added (e.g., 0.4). Also, like apo-$\beta$-rhMT, the 2+ and 3+ charge states decrease in intensity following addition of 1 equiv or more $Zn^{2+}$, relative to the 4+ charge state (compare the ESI-mass spectral data of apo-$\alpha$-rhMT to $Zn_4$-$\alpha$-rhMT). These changes in the overall charge state manifold profile demonstrate that the metalated forms of both $\beta$- and $\alpha$-rhMT, while similar to that of the apo-forms of the protein, occupy a somewhat larger volume.

We have assembled the relative abundances of each metalated $\alpha$-rhMT species (Figure 4) into Figure 5, which clearly demonstrates that partial metalation occurs; hence, the extent of metalation is directly dependent on the amount of $Zn^{2+}$ in solution. Figure 5A shows a top-down view of the linear progression of metalation from apo-$\alpha$-rhMT to $Zn_4$-$\alpha$-rhMT. This linearity is important because it demonstrates that metalation occurs in a noncooperative manner, where the declining affinity of $Zn^{2+}$ for $\alpha$-rhMT is directly related to the number of remaining, available metal-binding sites. Figure 5B demonstrates that at each equivalent of zinc, with the exception of the beginning and end of the titration, $\alpha$-rhMT exists as a mixture of metalated states. At low equivalents of $Zn^{2+}$ only partially metalated species are observed, while at excess equivalents (>4 equiv of $Zn^{2+}$) only the fully metalated $\alpha$-rhMT is observed. The slight increase in the fraction of $Zn_2$-$\alpha$-rhMT is clear in both the contour and bar graph, before $Zn_3$- and finally, $Zn_4$-rhMT form.

**Noncooperative Metalation of Isolated Apo-$\beta\alpha$-rhMT 1a by $Zn^{2+}$.** The mass spectral data recorded during the titration of apo-$\beta\alpha$-rhMT with $Zn^{2+}$ and the corresponding deconvoluted spectra are shown in Figure 6A–F. As is the case for both the isolated fragments containing the $\beta$- and $\alpha$-

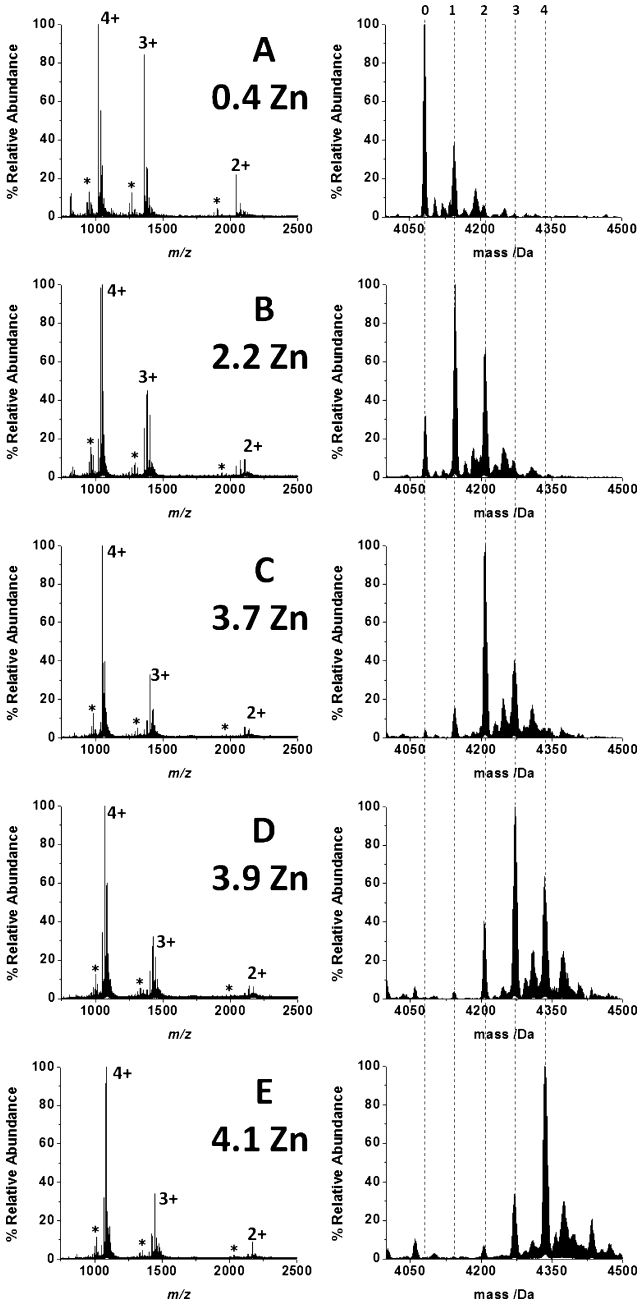


**Figure 4.** ESI mass spectra recorded during the titration of 34.1 $\mu$M apo-$\alpha$-rhMT 1a at pH 9.5, with $ZnSO_4$. Spectral changes were recorded as aliquots of Zn(II) (7.3 mM) were titrated into the solution held on ice. Mass spectral charge states of $\alpha$-rhMT (left) and their deconvoluted counterparts (right) were recorded at Zn(II) molar equivalents of 0.4, 2.2, 3.7, 3.9, and 4.1. Metalation in excess of $Zn_4$-$\alpha$-rhMT is a result of nonspecific adducts.

domains, stepwise metalation of apo-$\beta\alpha$-rhMT leads to the formation of partially metalated species (from $Zn_1$ to $Zn_6$) at substoichiometric equivalents ($\beta\alpha$ < 7 $Zn^{2+}$), confirming the noncooperative nature of the metalation reaction. The end point of the titration occurs after 7 equiv of $Zn^{2+}$ has been added to the solution and is likely the result of slight errors in the estimation of the apoprotein concentrations as well as the formation of trace amounts of competitive $Zn(OH)_2$ as a result of the high pH of the solution. Also, there is a small amount of dimer found around 2000 $m/z$ that corresponds to a 7+ charge


dx.doi.org/10.1021/bi3004523 | Biochemistry 2012, 51, 6690–6700

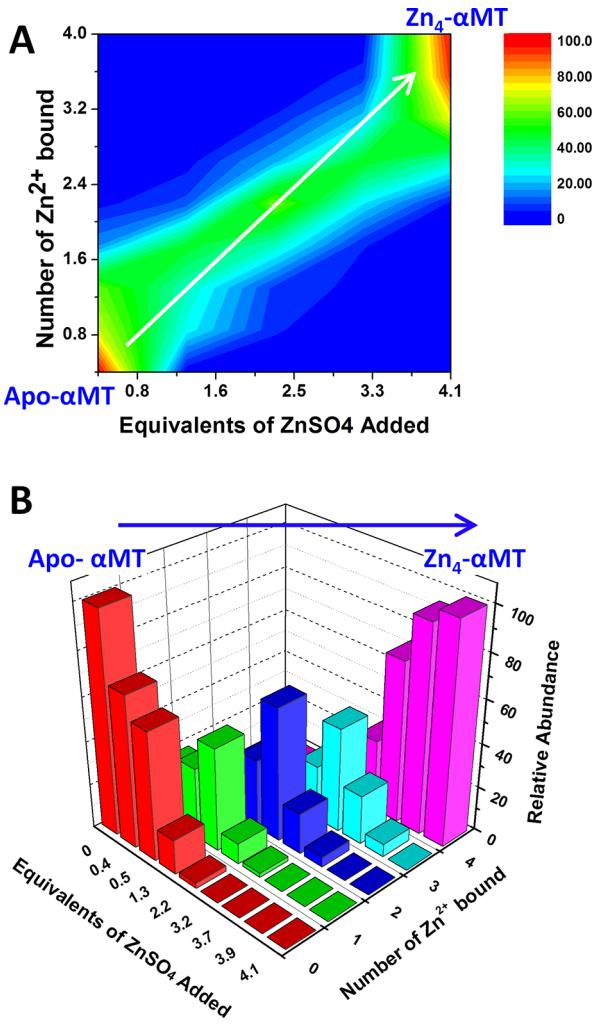


**Figure 5.** Contour and bar graph representation of the metalation state of $\alpha$-rhMT 1a as a function of Zn(II) added. (A) A top-down view of metalation, showing the linear progression from apo-$\alpha$-rhMT to $Zn_4$-$\alpha$-rhMT as a function of $Zn^{2+}$ added to solution. The adjacent legend ranges between 100% abundance (red) and 0% abundance (dark blue). (B) A side-on view of metalation, which shows the relative abundance of each species as a function of $Zn^{2+}$ added to the solution. Color code: apo-$\alpha$-rhMT is red; $Zn_1$-$\alpha$-rhMT is green; $Zn_2$-$\alpha$-rhMT is dark blue; $Zn_3$-$\alpha$-rhMT is light blue; $Zn_4$-$\alpha$-rhMT is purple. In both (A) and (B), as the amount of $Zn^{2+}$ added to the solution of apo-$\alpha$-rhMT 1a increases, the number of metals bound to $\alpha$-rhMT 1a also increases. $\alpha$-rhMT exists as a mixture of species, with the exception of the beginning and end of the titration. This graph is based on the deconvoluted mass spectral data shown in Figure 4.

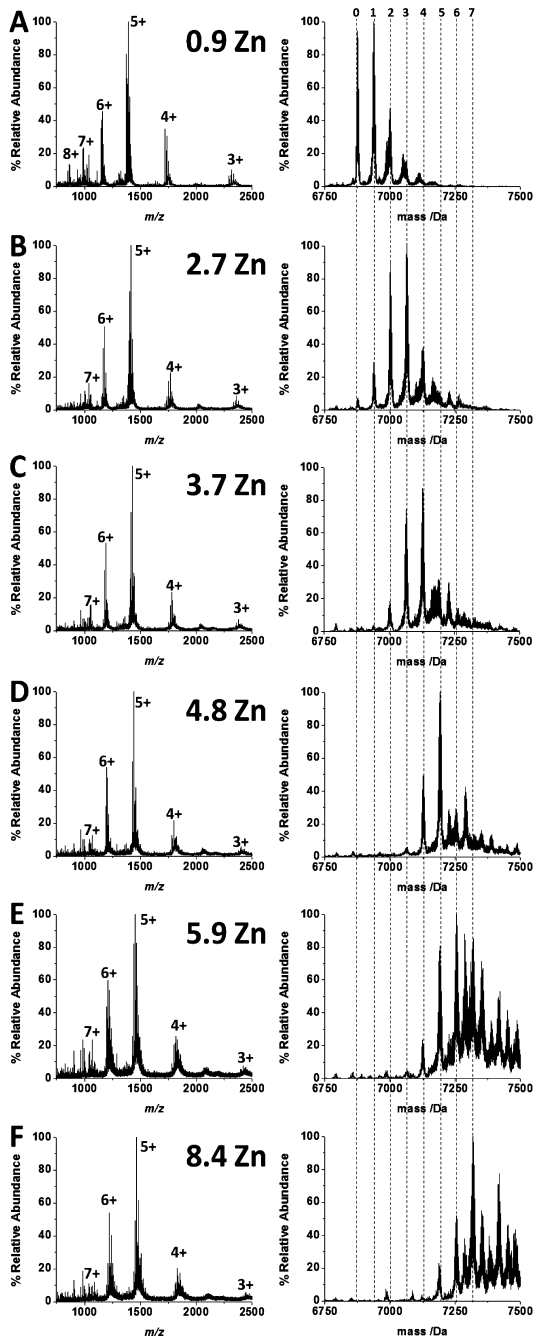


**Figure 6.** ESI mass spectra recorded during the titration of 29.2 $\mu$M apo-$\beta\alpha$-rhMT 1a at pH 9.1, with $ZnSO_4$. Spectral changes were recorded as aliquots of Zn(II) (7.3 mM) were titrated into the solutions on ice. Dotted lines follow metal binding. Mass spectral charge states of $\beta\alpha$-rhMT (left) and their deconvoluted counterparts (right) were recorded at Zn(II) molar equivalents of 0.9, 2.7, 3.7, 4.8, 5.9, and 8.4. The peak between $Zn_6$- and $Zn_7$-$\beta\alpha$-rhMT at 5.9 equiv of Zn(II) has been identified as $Zn_6$-$\beta\alpha$-rhMT with a chloride adduct bound. Metalation in excess of $Zn_7$-$\beta\alpha$-rhMT is a result of nonspecific adducts.

state and tracks with the number of $Zn^{2+}$ ions added to solution. It has not affected our calculations of equivalents. In each step of the titration, the dominant metalation state is a direct result of the number of equivalents of $Zn^{2+}$ added to solution. Apo-$\beta\alpha$-rhMT exhibits a charge state profile that ranges from 8+ to 3+. The increase in the total number of charge states, as compared to the isolated domains, is because the full protein occupies a larger volume than either of the two isolated domains. At 2.7 equiv of $Zn^{2+}$, the dominant metalation states are $Zn_2$- and $Zn_3$-$\beta\alpha$-rhMT. A significant reduction in the intensity of the 7+ charge state as well as the disappearance of the 8+ charge state is also observed at this point. These changes to the charge state manifold distribution suggest that the first metal ion must significantly restrict the motion of the protein reducing its volume. Beyond 2.7 equiv of $Zn^{2+}$, there is very little change in the 6+, 5+, 4+, and 3+ charge state distribution, indicating that further metalation does not substantially increase the folding of the protein.

We have assembled the relative abundances of each metalated $\beta\alpha$-rhMT species (Figure 6) into Figure 7, which clearly demonstrates that partial metalation occurs; hence, the


dx.doi.org/10.1021/bi3004523 | *Biochemistry* 2012, 51, 6690−6700

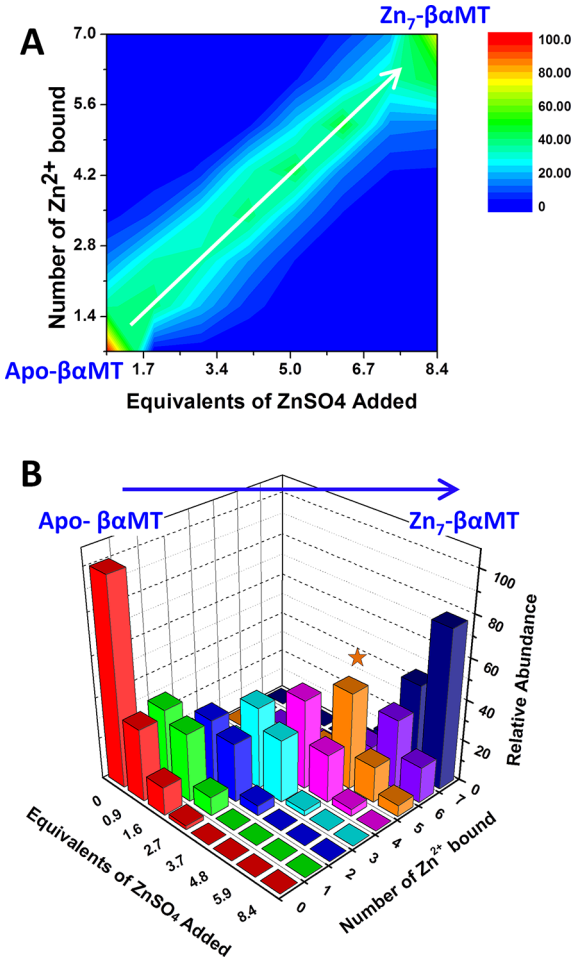


**Figure 7.** Contour and bar graph representaiton of the metalation state of $\beta\alpha$-rhMT 1a as a function of Zn(II) added. (A) A top-down view of metalation, showing the linear progression from apo-$\beta\alpha$-rhMT to $Zn_7$-$\beta\alpha$-rhMT as a function of $Zn^{2+}$ added to solution. The adjacent legend ranges between 100% abundance (red) and 0% abundance (dark blue). (B) A side-on view of metalation, which shows the relative abundance of each species as a function of $Zn^{2+}$ added to solution. Color code: apo-$\beta\alpha$-rhMT is red; $Zn_1$-$\beta\alpha$-rhMT is green; $Zn_2$-$\beta\alpha$-rhMT is dark blue; $Zn_3$-$\beta\alpha$-rhMT is light blue; $Zn_4$-$\beta\alpha$-rhMT is light purple; $Zn_5$-$\beta\alpha$-rhMT is orange; $Zn_6$-$\beta\alpha$-rhMT is violet; $Zn_7$-$\beta\alpha$-rhMT is indigo. In both (A) and (B), as the amount of $Zn^{2+}$ added to the solution of apo-$\beta\alpha$-rhMT 1a increases, the number of metals bound to $\beta\alpha$-rhMT 1a also increases. $\beta\alpha$-rhMT exists as a mixture of species, with the exception of the beginning and end of the titration. The star identifies the increased fraction of $Zn_5$-$\beta\alpha$-rhMT, which we describe in the text as having special stability. This graph is based upon the deconvoluted mass spectral data shown in Figure 6.

extent of metalation is directly dependent on the amount of metal in solution. Figure 7A shows a top-down view of the linear progression of metalation from apo-$\beta\alpha$-rhMT to $Zn_7$-$\beta\alpha$-rhMT. This linearity is important because it demonstrates that metalation occurs in a noncooperative manner, where the affinity of $Zn^{2+}$ for $\beta\alpha$-rhMT is directly related to the number of available metal-binding sites. Figure 7B demonstrates that at each equivalent of zinc, with the exception of the beginning and end of the titration, $\beta\alpha$-rhMT exists as a mixture of metalated states. At low equivalents of $Zn^{2+}$ only partially metalated species are observed, while at excess equivalents (>7 equiv of $Zn^{2+}$) only the fully metalated $\beta\alpha$-rhMT is observed. More clearly than for the metalation of the $\alpha$-rhMT or $\beta$-rhMT, a partially metalated species clearly intensifies with five $Zn^{2+}$ bound. $Zn_5$-rhMT exhibits a greater fraction than expected (the star in Figure 7B).

## DISCUSSION

MT is often implicated in metal-ion homeostasis, toxic metal detoxification, and as a protective agent against oxidative stress. MT has also been shown to act as a metallochaperone, capable of transporting essential metal ions, such as $Cu^{+}$ and $Zn^{2+}$ in a controlled manner. In this role, MT must be able to deliver these metal ions to apo-enzymes. Indeed, metal exchange experiments have been conducted in which $Zn^{2+}$ from $Zn_7$-$\beta\alpha$-MT has been transferred to Zn-dependent enzymes, for example, *m*-aconitase,[35] carbonic anhydrase,[36,37] and the prototypical transcription factor, Gal4.[38] Removal of $Zn^{2+}$ from the zinc finger-containing transcription factor Sp1 demonstrates that MT may also act as a $Zn^{2+}$ acceptor.[39] These reports show the metal donor and acceptor capabilities of MT. ESI−mass spectral studies have highlighted the stability of partially metalated MT, for example during the transfer of $Zn^{2+}$ from Zn-MT to metal ion chelators or to an apoenzyme.[40−42]

As a metalochaperone involved with zinc homeostasis, MT has also been implicated in the longevity of certain human groups.[43] In addition, the equilibria between apo-MT, oxidized MT, and holo-MT have been suggested to affect the stress response of organisms.[44] However, this mechanism has always assumed that metalation of MT occurs in a cooperative "all or nothing" fashion. The results presented in this study demonstrate that the metalation of MT with zinc, in fact, occurs in a noncooperative fashion and that these partially metalated species may be critical in the balance of metal ions. There has recently been a report of the isolation of partially oxidized MT from mice under oxidative stress, which further supports the role of partially metalated MT as a protective agent against oxidative stress.[45] Mutations of human MT have also been associated with hyperglycemia, ischemic cardiomyopathy, and both diabetes type 2 and related cardiovascular complications.[46−48] MT is able to impact the pathogenesis of these diseases through both Zn buffering and antioxidant dysfunction, which in turn rely on the metalation status *in vivo*. It is clear that knowledge of the mechanism of metalation is needed to establish the metal status *in vivo*, which will aid in determining the exact involvement of MT in these disorders.

The $Zn^{2+}$ metalation properties of the isolated fragments and full protein were determined using sensitive, soft ESI-MS methods (Figures 2−7). We must emphasize that the ESI-MS conditions must be very soft or metals may be lost distorting the interpretation. It is clear from the graphical representations of the data that the metalation proceeds without loss of $Zn^{2+}$. Through an analysis of the changes in the charge state manifold profile, the effect of the increasing metal content on protein folding was determined. The two isolated domains possess similar charge state manifolds throughout the titration, with a slight increase following binding the first $Zn^{2+}$ ion, after which the charge state distributions remain constant with the 4+ state dominating the metalated species in both fragments until fully metalated with $Zn^{2+}$. The prominent charge state for the apo-, two-domain, $\beta\alpha$-MT is 5+ with equal contributions from the 6+ and 4+ charge states. Metalation results in a small increase in 6+ and a reduction in 4+, suggesting that the apo- and metalated proteins are actually of quite similar volume. The


dx.doi.org/10.1021/bi3004523 | *Biochemistry* 2012, 51, 6690−6700

data show clearly that $Zn^{2+}$ metalation takes place stepwise for each protein.

By analyzing the distribution of metalated states for both the rhMT, and its isolated domains, we have shown that metalation occurs in a linear stepwise fashion, which strongly indicates that each metal binds in a noncooperative fashion (Figures 3, 5, and 7). Contrasting this mechanism is the work of Gehrig et al., who determined that metalation of MT isoform 2 proceeds in a cooperative manner.[22] To further emphasize that MT metalates in a noncooperative fashion, we have the plotted experimental metalation data of the full MT protein in terms of the "life" of each Zn species ($n$ = 0−7). This is the first time the individually metalated species have been identified as a function of the molar equivalents of the $Zn^{2+}$ added as far as we know. One aspect of this plot is that at each value of $Zn^{2+}$ added, from $n$ = 1 to $n$ = 6, a range of species simultaneously exist, meaning that techniques that cannot discriminate between species with different numbers of metals bound will simply average the data from several species with different metalated states. The results of course will not be the same as those reported here for the individually metalated species. We simulated metalation data for both a noncooperative (Figure 8A) and cooperative system (Figure 8B) mechanism. The simulated data are based on a series of linearly decreasing (noncooperative) or increasing (cooperative) binding constants for the metalation of MT by $Zn^{2+}$. In (A), the theoretical distribution of Zn-MT for a noncooperative mechanism of metalation shows the significant abundance of all partially metalated species as a function of $Zn^{2+}$ present in solution. In (B), the theoretical distribution of Zn-MT for a cooperative mechanism of metalation has been plotted. Critical to any cooperative mechanism is that the most abundant species at any given concentration of $Zn^{2+}$ is either the metal-free, apo-MT, or the fully metalated, $Zn_7$-MT. When compared to the experimental data (Figure 8C), it is clear that a noncooperative mechanism of metalation is in effect for the binding of $Zn^{2+}$ ions to the MT. With the exception of the very early stages of metalation (<1 equiv), and the very late stages of metalation (>6.5 equiv), neither the metal-free nor the fully metalated species dominate. Consequently, on the basis of a comparison of the experimental data with the simulated data, we must conclude that MT metalates $Zn^{2+}$ in a noncooperative fashion.

While our results conclusively show that the mechanism of metalation of MT for $Zn^{2+}$ is noncooperative, we cannot rule out the possibility these results may be isoform specific; that is, MT 1a metalates noncooperatively with $Cd^{2+}$ and $As^{3+}$ (from previous reports), and now $Zn^{2+}$, but from previous reports MT 2a metalates cooperatively with $Zn^{2+}$, $Cd^{2+}$, and $Cu^{+}$. New experimental studies are required to determine whether cooperativity for MT 2a is an isoform-dependent property. More recently, significant differences in the metalation chemistry of the MT isoforms have been established, including the ability of both MT 1a and 3 to bind an eighth $Cd^{2+}$ ion forming the supermetalated $Cd_8$-$\beta\alpha$-rhMT, while MT 2 is only able to bind seven $Cd^{2+}$ ions forming $Cd_7$-$\beta\alpha$-rhMT. Taken together, these results suggest that each MT isoform may have a specific cellular function.

One noteworthy point is the stability of $Zn_5$-$\beta\alpha$-rhMT (Figures 6D, 7B, and 8C). At the 4.8 $Zn^{2+}$ point in the titration, the spectra are significantly simplified with only $Zn_5$- and ~33% $Zn_4$-$\beta\alpha$-rhMT. This simplification in the number of species suggests that the association constant ($K_F$) of $Zn_6$-$\beta\alpha$-rhMT is significantly weaker than that of $Zn_5$-$\beta\alpha$-rhMT so that excess

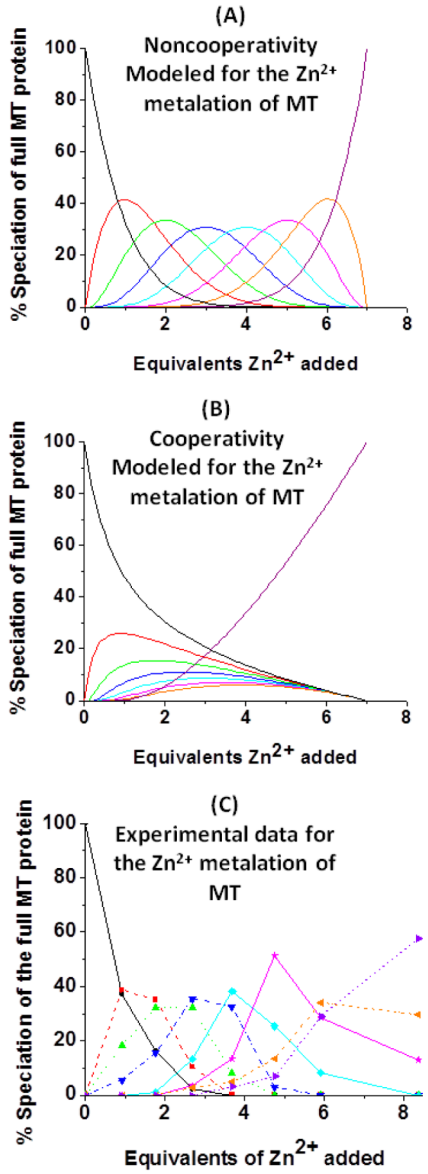


**Figure 8.** Models and experimental data showing $Zn^{2+}$ speciation during metalation of the full MT protein. (A) A model using noncooperativity rules (declining $K_F$'s) of ESI-MS data based upon a series of linearly decreasing association constants. (B) A model using cooperativity rules (increasing $K_F$'s) of ESI-MS data based upon a series of linearly increasing association constants. (C) Experimental ESI-MS data for the metalation of apo-$\beta\alpha$-rhMT 1a. Each line corresponds to a different metalation state: $Zn_0$ (black circle), $Zn_1$ (red square), $Zn_2$ (green triangle), $Zn_3$ (blue triangle), $Zn_4$ (light blue diamond), $Zn_5$ (magenta star), $Zn_6$ (orange triangle), and $Zn_7$ (purple triangle).

$Zn^{2+}$ must be added to bind the sixth $Zn^{2+}$. While the exact reason for the drop is uncertain at this time, we propose that at the 5 $Zn^{2+}$ point each of the five $Zn^{2+}$ ions is coordinated to 4 terminal cysteine residues and that binding of the sixth $Zn^{2+}$ ion requires a rearrangement of these residues to form the first part of the expected 2-domain structure. This model is extremely important in the determination of the metal-ion distribution during metalation of the apoprotein. The model simply says that the 5 $Zn^{2+}$ shall be coordinated terminally using all 20 cysteine thiols before clustering takes place. Therefore, the two-domain structure does not begin to take form until the sixth


dx.doi.org/10.1021/bi3004523 | *Biochemistry* 2012, 51, 6690−6700

$Zn^{2+}$ is bound. There is substantial evidence that the terminally coordinated metals are present before clustering takes place for metals for which spectroscopic probes are available. Several papers have reported monitoring metalation titrations using a range of techniques, including $^{113}$Cd-NMR, Co-EPR, and CD spectroscopies, and have concluded that the initial metalation of MT occurs exclusively via terminal cysteine residues, after which cluster formation leads to bridging interactions.[49−51]

One possible alternative to the existence of a $Zn_5$ species consisting solely of terminally coordinated $Zn^{2+}$ ions is that a single $Zn^{2+}$ ion binds in the $\beta$-domain and four $Zn^{2+}$ bind cooperatively, and in a domain-specific manner, in the $\alpha$-domain. While there have been reports of spectroscopic data interpreted in terms of a domain-specific, cooperative mechanism resulting in the complete saturation of one domain before cysteines of the sequence that would form the second domain bind, we feel that the thermodynamic argument supports our interpretation of the mass spectral data for the hMT1 protein studied here. That is, terminally bound thiols (cysSH) exhibit shorter bond lengths than their bridged analogues and, therefore, are energetically more favorable. In our view, a complex involving 20 terminal cysS-$Zn^{2+}$ bonds in a chain of 5{$Zn(Scys)_4^{2-}$} units will be thermodynamically more favorable than {$[Zn_4(Scys)_{11}]^{3-}$ + $Zn(Scys)_4^{2-}$ + 5cysSH} (two identical molecular systems, with just the $Zn^{2+}$ complexes rearranged).

A different interpretation of experimental data was reported for a $Cd^{2+}$ titration of rabbit liver MT 2 monitored by NMR spectroscopy in which it was proposed that these data demonstrated the exclusive saturation of the $\alpha$-domain, after which the $\beta$-domain was populated.[49] In that same NMR experiment a broad featureless peak centered at 688 ppm also existed during the titration that could have been a $Cd_5$-MT species with significant fluctionality due to the exclusively terminal coordination of $Cd^{2+}$ to cysteine. Until the $Cd^{2+}$ experimental is repeated using mass spectrometry to confirm the metal speciation as a function of metal loading, we cannot rule out the possibility that for $Cd^{2+}$ binding to MT2 there may be domain specific, cooperative binding at the high concentrations used in the NMR experiment. At much lower concentrations (~10 $\mu$M) we have previously reported for human MT1a that $Cd^{2+}$ binds noncooperatively.[24,52]

Finally, the recent kinetic studies of $As^{3+}$ metalation of hMT1 demonstrated conclusively that the affinity of MT for $As^{3+}$ is directly dependent upon the number of available metal binding sites,[2,25,28] with the specific rate constants declining linearly as the number of $As^{3+}$ bound increased forming a chain of cys-coordinated 6($AsS_3$). For a cooperative mechanism, the specific rate constants would increase for each successive $As^{3+}$ bound. The data in this present report indicate a similar mechanism, which means that the binding is noncooperative and domains form only for the sixth and seventh $Zn^{2+}$ added.

Analogous to $Zn_5$-MT, a four copper folding intermediate, $Cu_4$-MT, has also been reported to have special stability.[21] As with $Zn_5$-MT, it is likely that the conversion of $Cu_4$-MT to $Cu_5$-MT requires the bridging of cysteine residues, which greatly affects the association constants. Unlike the zinc titration reported herein, the $Cu_4$ formation is reported to occur in a cooperative manner. Since both copper and zinc are the two biologically relevant metal ions in metallothionein chemistry, it is possible that this difference in the mechanism of metalation may be the crucial cellular differentiation property of the differently metalated MT species.[3]

MT is often cited as a protective agent against oxidative stress, where the balance between the metalated MT and the metal free MT mediates the redox chemistry of the cell.[29,44,53] This view does not take into account the noncooperative nature of the metalation of metallothionein with zinc. It is likely that the average metal load of MT is what dictates the oxidative environment of the cell. DFT calculations of the reactivity of polynuclear zinc−thiolate sites have shown the mononuclear $ZnCys_4$ moiety to be more nucleophilic than either of the two fully metalated $Zn_3Cys_9$ and $Zn_4Cys_{11}$ clusters.[54] Given this information and the work presented here and even though $Zn_5$-$\beta\alpha$-rhMT possesses no free thiol groups, $Zn_5$-MT should be able to take part in cellular chemistry as a protecting agent against oxidative stress.

With a noncooperative mechanism of metalation now established for the biologically relevant zinc, we may suggest that partially metalated species may be stable and able to take part in cellular chemistry. Consequently, instances in which partially metalated forms of the protein have been purified could in fact represent the biologically relevant *in vivo* forms of the protein.[45] In addition, the 20 cysteine residues present in mammalian MT have long made it an attractive agent to combat oxidative stress with concomitant formation of disulfide bonds.[29] In both cases, MT can now be understood to be able to combat oxidative stress in a dynamic way, where progressive oxidation of MT leads to the sequential release of $Zn^{2+}$ ions and eventually complete oxidation. This released $Zn^{2+}$ can then bind to the metal response element binding transcription factor 1 (MTF-1).[55] Zn-MTF-1 leads to an upregulation of MT, and other associated proteins, thus combating the oxidative stress. Future work will include a re-evaluation of the isolation of partially metalated MT and the stability of partially metalated forms of the protein when exposed to oxidative stress.

## ■ CONCLUSIONS

In this study, we demonstrate that $Zn^{2+}$ metalation occurs in a noncooperative manner in the same way as for the less biologically relevant $Cd^{2+}$ and $As^{3+}$ but in contrast to the essential $Cu^{+}$ reported previously. From our report it is now clear that one of the two most relevant metals in the metallothionein biological chemistry metalates in a non-cooperative manner. We show that there exists a stable $Zn_5$-$\beta\alpha$-rhMT species, which is likely to include only terminal thiolates bound to isolated $Zn^{2+}$ ions in a series of $ZnS_4$ groups spread along the peptide chain. The enhanced stability of this species is probably the result of the switch from terminal to bridging Cys, which reduces the associated affinity of the protein for $Zn^{2+}$. While domain specificity may exist, and zinc may initially bind preferentially at either the C-terminus (eventually the $\alpha$-domain) or the N-terminus (eventually the $\beta$-domain), there is probably no domain formation. Identification of the first cysteines to bind the $Zn^{2+}$ is clearly a future goal.

## ■ AUTHOR INFORMATION

### Corresponding Author

*Tel 1-519-661-3821; Fax 1-519-661-3022; e-mail Martin.Stillman@uwo.ca.

### Funding

We thank NSERC of Canada and the Academic Development Fund at The University of Western Ontario for financial support through operating funds (to M.J.S.), Fujitsu, Poland,

for the Scigress license support, and an Alexander Graham Bell Canada Graduate Scholarship (CGS) (to D.E.K.S.).

### Notes

The authors declare no competing financial interest.

## ■ ACKNOWLEDGMENTS

We thank Mr. Doug Hairsine for technical assistance.

## ■ ABBREVIATIONS

MT, metallothionein; $\beta$-rhMT 1a, recombinantly prepared beta domain of human metallothionein isoform 1a; $\alpha$-rhMT 1a, recombinantly prepared alpha domain of human metallothionein isoform 1a; $\beta\alpha$-rhMT 1a, recombinantly prepared human metallothionein isoform 1a; ESI, electrospray ionization; MS, mass spectrometry.

## ■ REFERENCES

(1) Nielson, K. B., Atkin, C. L., and Winge, D. R. (1985) Distinct metal-binding configurations in metallothionein. *J. Biol. Chem. 260*, 5342−5350.

(2) Ngu, T. T., and Stillman, M. J. (2006) Arsenic binding to human metallothionein. *J. Am. Chem. Soc. 128*, 12473−12483.

(3) Sutherland, D. E. K., and Stillman, M. J. (2011) The "magic numbers" of metallothionein. *Metallomics 3*, 444−463.

(4) Stillman, M. J. (1995) Metallothioneins. *Coord. Chem. Rev. 144*, 461−511.

(5) Robbins, A. H., McRee, D. E., Williamson, M., Collett, S. A., Xuong, N. H., Furey, W. F., Wang, B. C., and Stout, C. D. (1991) Refined crystal structure of Cd, Zn metallothionein at 2.0 Å resolution. *J. Mol. Biol. 221*, 1269−1293.

(6) Messerle, B. A., Schaffer, A., Vasak, M., Kagi, J. H. R., and Wuthrich, K. (1992) Comparison of the solution conformations of human [$Zn_7$]-metallothionein-2 and [$Cd_7$]-metallothionein-2 using nuclear magnetic resonance spectroscopy. *J. Mol. Biol. 225*, 433−443.

(7) Messerle, B. A., Schaffer, A., Vasak, M., Kagi, J. H. R., and Wuthrich, K. (1990) Three-dimensional structure of human [$^{113}Cd_7$]-metallothionein-2 in solution determined by nuclear magnetic resonance spectroscopy. *J. Mol. Biol. 214*, 765−779.

(8) Zangger, K., Oz, G., Otvos, J. D., and Armitage, I. M. (1999) Three-dimensional solution structure of mouse [$Cd_7$]-metallothionein-1 by homonuclear and heteronuclear NMR spectroscopy. *Protein Sci. 8*, 2630−2638.

(9) Sutherland, D. E. K., Willans, M. J., and Stillman, M. J. (2012) Single domain metallothioneins: Supermetalation of human MT 1a. *J. Am. Chem. Soc. 134*, 3290−3299.

(10) Meloni, G., Polanski, T., Braun, O., and Vasak, M. (2009) Effects of $Zn^{2+}$, $Ca^{2+}$, and $Mg^{2+}$ on the structure of $Zn_7$metallothionein-3: Evidence for an additional zinc binding site. *Biochemistry 48*, 5700−5707.

(11) Briggs, R. W., and Armitage, I. M. (1982) Evidence for site-selective metal binding in calf liver metallothionein. *J. Biol. Chem. 257*, 1259−1262.

(12) Salgado, M. T., and Stillman, M. J. (2004) $Cu^+$ distribution in metallothionein fragments. *Biochem. Biophys. Res. Commun. 318*, 73−80.

(13) Meloni, G., Faller, P., and Vasak, M. (2007) Redox silencing of copper in metal-linked neurodegenerative disorders. *J. Biol. Chem. 282*, 16068−16078.

(14) Meloni, G., Sonois, V., Delaine, T., Guilloreau, L., Gillet, A., Teissie, J., Faller, P., and Vasak, M. (2008) Metal swap between $Zn_7$-metallothionein-3 and amyloid-$\beta$-Cu protects against amyloid-$\beta$ toxicity. *Nat. Chem. Biol. 4*, 366−372.

(15) Chan, J., Huang, Z., Watt, I., Kille, P., and Stillman, M. J. (2007) Characterization of the conformational changes in recombinant human metallothioneins using ESI-MS and molecular modeling. *Can. J. Chem. 85*, 898−912.

(16) Ngu, T. T., Sturzenbaum, S. R., and Stillman, M. J. (2006) Cadmium binding studies to the earthworm *Lumbricus rubellus* metallothionein by electrospray mass spectrometery and circular dichroism spectroscopy. *Biochem. Biophys. Res. Commun. 351*, 229−233.

(17) Merrifield, M. E., Chaseley, J., Kille, P., and Stillman, M. J. (2006) Determination of the Cd/S cluster stoichiometry in *Fucus vesiculosus* metallothionein. *Chem. Res. Toxicol. 19*, 365−375.

(18) Pan, P. K.-y., Zheng, Z. F., Lyu, P. C., and Huang, P. C. (1999) Why reversing the sequence of the $\alpha$ domain of human metallothionein-2 does not change its metal-binding and folding characteristics. *Eur. J. Biochem. 266*, 33−39.

(19) Jiang, L.-J., Maret, W., and Vallee, B. L. (1998) The glutathione redox couple modulates zinc transfer from metallothionein to zinc-depleted sorbitol dehydrogenase. *Proc. Natl. Acad. Sci. U. S. A. 95*, 3483−3488.

(20) Jacob, C., Maret, W., and Vallee, B. L. (1998) Control of zinc transfer between thionein, metallothionein, and zinc proteins. *Proc. Natl. Acad. Sci. U. S. A. 95*, 3489−3494.

(21) Jensen, L. T., Peltier, J. M., and Winge, D. R. (1998) Identification of a four copper folding intermediate in mammalian copper metallothionein by electrospray ionization mass spectrometry. *J. Biol. Inorg. Chem. 3*, 627−631.

(22) Gehrig, P. M., You, C., Dallinger, R., Gruber, C., Brouwer, M., Kagi, J. H. R., and Hunziker, P. E. (2000) Electrospray ionization mass spectrometry of zinc, cadmium, and copper metallothioneins: Evidence for metal-binding cooperativity. *Protein Sci. 9*, 395−402.

(23) Palumaa, P., Eriste, E., Njunkova, O., Pokras, L., Jornvall, H., and Sillard, R. (2002) Brain-specific metallothinein-3 has higher metal-binding capacity than ubiquitous metallothioneins and binds metals noncooperatively. *Biochemistry 41*, 6158−6163.

(24) Sutherland, D. E. K., and Stillman, M. J. (2008) Noncooperative cadmium(II) binding to human metallothionein 1a. *Biochem. Biophys. Res. Commun. 372*, 840−844.

(25) Ngu, T. T., Easton, A., and Stillman, M. J. (2008) Kinetic analysis of arsenic-metalation of human metallothionein: Significance of the two-domain structure. *J. Am. Chem. Soc. 130*, 17016−17028.

(26) Ngu, T. T., and Stillman, M. J. (2009) Metal-binding mechanisms in metallothioneins. *Dalton Trans.*, 5425−5433.

(27) Ngu, T. T., Lee, J. A., Rushton, M. K., and Stillman, M. J. (2009) Arsenic metalation of seaweed *Fucus vesiculosus* metallothionein: The importance of the interdomain linker in metallothionein. *Biochemistry 48*, 8806−8816.

(28) Ngu, T. T., Lee, J. A., Pinter, T. B. J., and Stillman, M. J. (2010) Arsenic-metalation of triple-domain human metallothioneins: Support for the evolutionary advantage and interdomain metalation of multiple-metal-binding domains. *J. Inorg. Biochem. 104*, 232−244.

(29) Kang, Y. J. (2006) Metallothionein Redox Cycle and Function. *Exp. Biol. Med. 231*, 1459−1467.

(30) Zhang, B., Georgiev, O., Hagmann, M., Gunes, C., Cramer, M., Faller, P., Vasak, M., and Schaffner, W. (2003) Activity of metal-responsive transcription factor 1 by toxic heavy metals and $H_2O_2$ in vitro is modulated by metallothionein. *Mol. Cell. Biol. 23*, 8471−8485.

(31) Krezel, A., and Maret, W. (2007) Dual nanomolar and picomolar Zn(II) binding properties of metallothionein. *J. Am. Chem. Soc. 129*, 10911−10921.

(32) Ejnik, J., Robinson, J., Zhu, J., Forsterling, H., Shaw-III, C. F., and Petering, D. H. (2002) Folding pathway of apo-metallothionein induced by $Zn^{2+}$, $Cd^{2+}$ and $Co^{2+}$. *J. Inorg. Biochem. 88*, 144−152.

(33) Felitsyn, N., Peschke, M., and Kebarle, P. (2002) Origin and number of charges observed on multiply-protonated native proteins produced by ESI. *Int. J. Mass Spectrom. 219*, 39−62.

(34) Kebarle, P., and Verkerk, U. H. (2009) Electrospray: From ions in solution to ions in the gas phase, what we know now. *Mass Spectrom. Rev. 28*, 898−917.

(35) Feng, W., Cai, J., Pierce, W. M., Franklin, R. B., Maret, W., Benz, F. W., and Kang, Y. J. (2005) Metallothionein transfers zinc to mitochondrial aconitase through a direct interaction in mouse hearts. *Biochem. Biophys. Res. Commun. 332*, 853−858.

(36) Mason, A. Z., Perico, N., Moeller, R., Thrippleton, K., Potter, T., and Lloyd, D. (2004) Metal donation and apo-metalloenzyme activation by stable isotopically labeled metallothionein. *Mar. Environ. Res. 58*, 371−375.
(37) Li, T.-Y., Kraker, A. J., Shaw-III, C. F., and Petering, D. H. (1980) Ligand substitution reactions of metallothioneins with EDTA and apo-carbonic anhydrase. *Proc. Natl. Acad. Sci. U. S. A. 77*, 6334−6338.
(38) Maret, W., Larsen, K. S., and Vallee, B. L. (1997) Coordination dynamics of biological zinc "clusters" in metallothioneins and in the DNA-binding domain of the transcription factor Gal4. *Proc. Natl. Acad. Sci. U. S. A. 94*, 2233−2237.
(39) Zeng, J., Heuchel, R., Schaffner, W., and Kagi, J. H. R. (1991) Thionein(apometallothionein) can modulate DNA binding and transcription activation by zinc finger containing factor Sp1. *FEBS Lett. 279*, 310−312.
(40) Zaia, J., Fabris, D., Wei, D., Karpel, R. L., and Fenselau, C. (1998) Monitoring metal ion flux in reactions of metallothionein and drug-modified metallothionein by electrospray mass spectrometry. *Protein Sci. 7*, 2398−2404.
(41) Leszczyszyn, O. I., and Blindauer, C. A. (2010) Zinc transfer from the embryo-specific metallothionien $E_c$ from wheat: a case study. *Phys. Chem. Chem. Phys. 12*, 13408−13418.
(42) Leszczyszyn, O. I., Evans, C. D., Keiper, S. E., Warren, G. Z. L., and Blindauer, C. A. (2007) Differential reactivity of individual zinc ions in clusters from bacterial metallothioneins. *Inorg. Chim. Acta 360*, 3−13.
(43) Mocchegiani, E., Giacconi, R., Muti, E., Cipriano, C., Costarelli, L., Tesei, S., Gasparini, N., and Malavolta, M. (2007) Zinc-bound metallothioneins and immune plasticity: lessons from very old mice and humans. *Immun. Ageing 4*, 1−8.
(44) Krezel, A., and Maret, W. (2007) Different redox states of metallothionein/thionein in biological tissue. *Biochem. J. 402*, 551−558.
(45) Feng, W., Benz, F. W., Cai, J., Pierce, W. M., and Kang, Y. J. (2006) Metallothionein disulfides are present in metallothionein-overexpressing transgenic mouse heart and increase under conditions of oxidative stress. *J. Biol. Chem. 281*, 681−687.
(46) Maret, W. (2008) A role for metallothionein in the pathogenesis of diabetes and its cardiovascular complications. *Mol. Genet. Metab. 94*, 1−3.
(47) Giacconi, R., Bonfigli, A. R., Testa, R., Sirolla, C., Cipriano, C., Marra, M., Muti, E., Malavolta, M., Costarelli, L., Piacenza, F., Tesei, S., and Mocchegiani, E. (2008) +647 A/C and +1245 MT1A polymorphisms in the susceptibility of diabetes mellitus and cardiovascular complications. *Mol. Genet. Metab. 94*, 98−104.
(48) Giacconi, R., Cipriano, C., Muti, E., Costarelli, L., Maurizio, C., Saba, V., Gasparini, N., Malavolta, M., and Mocchegiani, E. (2005) Novel-209A/G MT2A polymorphism in old patients with type 2 diabetes and atherosclerosis: relationships with inflammation (IL-6) and zinc. *Biogerontology 6*, 407−413.
(49) Good, M., Hollenstein, R., Sadler, P. J., and Vasak, M. (1988) $^{113}$Cd NMR studies on metal-thiolate cluster formation in rabbit Cd(II)-metallothionein: Evidence for a pH Dependence. *Biochemistry 27*, 7163−7166.
(50) Vasak, M., and Kagi, J. H. R. (1981) Metal thiolate clusters in cobalt(II)-metallothionein. *Proc. Natl. Acad. Sci. U. S. A. 78*, 6709−6713.
(51) Willner, H., Vasak, M., and Kagi, J. H. R. (1987) Cadmium-thiolate clusters in metallothionein: Spectrophotometric and spectropolarimetric features. *Biochemistry 26*, 6287−6292.
(52) Rigby-Duncan, K. E., and Stillman, M. J. (2007) Evidence for noncooperative metal binding to the $\alpha$ domain of human metallothionein. *FEBS J. 274*, 2253−2261.
(53) Petering, D. H., Zhu, J., Krezoski, S., Meeusen, J., Kiekenbush, C., Krull, S., Specher, T., and Dughish, M. (2006) Apo-metallothionein emerging as a major player in the cellular activities of metallothionein. *Exp. Biol. Med. 231*, 1528−1534.
(54) Ohanessian, G., Picot, D., and Frison, G. (2011) Reactivity of polynuclear zinc-thiolate sites. *Int. J. Quantum Chem. 111*, 1239−1247.
(55) Chen, X., Chu, M., and Giedroc, D. P. (1999) MRE-binding transcription factor-1: Weak zinc-binding finger domains 5 and 6 modulate the structure, affinity, and specificity of the metal-response element complex. *Biochemistry 38*, 12915−12925.